A high-throughput maize kernel traits scorer based on line-scan imaging

Xiuying Liang [a,c], Ke Wang [a], Chenglong Huang [a,c], Xuehai Zhang [b], Jianbing Yan [b], Wanneng Yang [a,b,c,*]

[a] College of Engineering, Huazhong Agricultural University, Wuhan 430070, PR China
[b] National Key Laboratory of Crop Genetic Improvement, Huazhong Agricultural University, Wuhan 430070, PR China
[c] Agricultural Bioinformatics Key Laboratory of Hubei Province, Huazhong Agricultural University, Wuhan 430070, PR China

ARTICLE INFO

ABSTRACT

Maize kernel traits such as kernel length, kernel width and kernel number determine kernel weight and, consequently, maize yield. Therefore, the measurement of kernel traits is important for maize breeding and the evaluation of maize yield. The conventional method for measuring kernel traits is still manual, which is time consuming, costly and subjective. In this study, a novel maize kernel traits scorer (MKTS) was developed for the automatic measurement of 12 maize kernel traits based on line-scan imaging, image processing, and automatic control techniques. Here, total of 615 samples were measured to evaluate the system performance. The results showed that the MKTS was capable of evaluating maize kernel traits with the mean absolute percentage error of the manual and automatic measurements less than 5% and the measurement efficiency of approximately 72 s for the measurement of 6 ears. In conclusion, this high-throughput scorer will provide maize scientists with a novel tool to assist in maize functional genetics and maize breeding.

1. Introduction

Maize (*Zea mays* L.) is a primary food, feed and fuel worldwide [1,2]. To meet the demands of the world's growing population, improvement in maize yield and quality through the combination of traditional and molecular breeding is urgently needed [2]. Kernel traits are important in maize breeding programs. Such traits include kernel yield [3], which is determined by the ear number per plant, the kernel number per ear and the kernel weight [4–6]. The kernel weight is one of the most important agronomic traits; it is determined by kernel shape, including the kernel length, kernel width, and kernel thickness [7]. With the development of next generation sequencing technologies, the generation of high quality genotype data has become extremely feasible in maize. To dissect the genetic basis of maize kernel traits, the accurate measurement of maize kernel traits is crucial and advantageous in functional genomics research and genetic improvement in maize.

The conventional method for measuring and recording maize kernel traits is still manual, which is time consuming, costly, and subjective [8,9]. Plant phenomics is a multidisciplinary field that combining of mechanics, automatic control, photonics-based techniques, and digital image processing to plant science study [10]. Digital imaging has been widely used in agriculture, such as in the detection of rice yield-related traits [7,11], the determination of the surface color of agricultural products [12–14], the detection mechanical damage in kernels [12,15,16], locating insects in cereal grains [17], mapping of seed shape/size QTL [4–6,18], and the evaluation of grain quality [19–23]. For maize, phenomics is used to evaluate the quality of kernels, classify maize kernels into size categories, and measure kernel shape. Valiente-Gonzalez [24] designed a computer vision system to capture single dent corn kernels and determine whether kernels were damaged using a principal component analysis (PCA) algorithm. Xun et al. [25] developed an on-line seed grading system based on machine vision; corn seeds were sorted into four grades according to morphological parameters, with an average eligible grading ratio of 81.90%. Steen-hoek and Precetti [26] evaluated the use of two-dimensional image analysis for the classification of maize kernels according to size with accuracy greater than 96% for round-hole decisions and less

than 80% for flatness decisions. Ni et al. [27] developed an electronic corn kernel size grading system based on machine vision and measured kernel length, width and projected area. However, the kernels were individually measured in stationary way, and the processing time was between 2.03 and 2.09 s per kernel. Severini et al. [28] developed a method for counting maize kernels using the open source software ImageJ, but maize kernels were spread over the sample platform by hand. Recently, with manual spreading samples, some researchers measure particle shape/size using image processing software such as ImageJ and SmartGrain. Igathinathane et al. [29] developed an ImageJ plugin to identify disjoint particles shape and determine their particles size distribution. Tanabata et al. [30] developed SmartGrain software for high-throughput measurement of seed shape. To the best of our knowledge, little effort has been undertaken for the high-throughput extraction of maize kernel traits in commercialized products.

In this study, automatic control and image analysis techniques based on line-scan imaging were used to develop a high-throughput maize kernel traits scorer (MKTS) to measure maize kernel traits. These traits included ear number (EN), kernel length (KL), kernel width (KW), the length-width ratio (LWR), kernel projected area (KPA), kernel projected perimeter (KPP), the total kernel number (TKN), the total kernel weight (TKW), the weight per 100 kernels (100-KW), the kernel weight per ear (KWPE), the kernel number per ear (KNPE), and roundness. Equipped with image processing and automatic control technologies, this novel instrument provided a high-throughput and high-accuracy method for maize kernel scoring, and has potential to be popularized in maize functional genetics, genomics and breeding.

2. Materials and methods

2.1. Materials

In this study, a total of 615 different maize samples were used in this study. From these 615 samples, 20 maize kernels with uniform areas were chosen to evaluate the system performance for measuring the kernel shape (KL, KW, and LWR) and the other remaining kernels were used to evaluate the system performance for measuring the TKN, TKW, and 100-KW. For the manual measurement of the KL and KW, the length and width of each kernel of 20 maize kernels with uniform areas were measured with three people using a digital vernier caliper, and the average value was calculated. For the manual measurement of TKN, each sample was counted with three people and the average was calculated. After measured manually, all the 615 maize samples were measured automatically using the MKTS system. Moreover, 10 different maize samples were chosen randomly from the 615 samples to validate the repeatability of the MKTS. The experimental design was show in the Supplementary file 1.

2.2. System description

The user operation area and a prototype of the system are shown in Fig. 1a. The operation area included a software interface, a barcode scanner, a feeding interface and a vibrating feeder. When maize kernels were manually placed in the feeding interface, the samples were delivered to the inspection unit (Fig. 1b) by the vibrating feeder. The inspection unit was designed with the following three key components: a line-scan camera with short-focus lens, a line-array LED light source and a conveyor with a servo motor. To acquire maize kernel images continuously and shorten image processing time, a line scan camera was applied instead of a conventional frame camera because merging kernel images is easier with a line scan camera than that of frame camera. To achieve high-throughput and dynamic measurements, an industrial conveyor driven by the servo motor, which was blackened to enhance contrast between the maize kernels and the background, delivered maize kernels through the imaging area automatically. The two line-array LED light sources provided uniform illumination. The inner layout of the system is illustrated in Fig. 1c; this included the inspection unit, a power adapter for the light source, a programmable logic controller (PLC), a computer, a feeder driver, an electronic scale and a collection box. The feeder control, the conveyor control and communication with computer were achieved via the PLC. The collection box was used to collect the measured maize kernels. The TKW was obtained via the electronic scale. The details of the component used in the maize kernel traits scorer (MKTS) were shown in the Supplementary file 2. The operation procedure video of the MKTS was shown in the Supplementary file 3.

2.3. Operation procedure and system controls

The system operation procedure (shown in Fig. 2a) included the following steps: (1) Start the system and scan the barcode; (2) input the ear number; (3) put the kernels into the feeding interface and start the inspection; (4) allow each frame image to be acquired and delivered to the queue for image processing; (5) after all the kernels were scanned, end the current task and acquire the total kernel weight with the electronic scale; and (6) find the results, including the original gray image and the maize kernel traits, stored in the user-predefined folder. The PLC was programmed using CX-Programmer 7.3 (Omron, Japan), the software for the computer was developed using LabVIEW 8.6 (National Instruments, USA), and the software for statistics analysis of maize kernel traits was SPSS (version 19.0, International Business Machines Corporation, USA).

2.4. Image processing and the extraction of traits

A flow chart of the image processing used for the measurement of maize kernel traits is outlined in Fig. 2b. After each kernel was captured by the line-array camera, the kernel images were sent to a queue. Image processing was synchronous with image acquisition, which included the following steps: (1) N frame images were fetched from the queue and a non-adaptive thresholding algorithm (the threshold value was 10) was applied to divide the gray image into a background and foreground for each image frame; then several morphological operators (including open and filling holes) were used to process the binary image; (2) the processed image was split into two parts, including a cut part and a remaining part; (3) the remaining part of the N image was merged with the cut part of the former image to obtain a merged image; (4) the mean value of the projected area (MVPA) of all objects was obtained and the objects with a projected area less than 0.4 times the MVPA were not considered as maize kernels and removed using particle filter operator; (5) then the Elongation Factor for all kernel samples (1.4–3.4), which was defined as maximum diameter divided by equivalent rectangle short side, was calculated and the objects with Elongation Factor more than 4 were not considered as maize kernels and removed using particle filter operator; (6) the projected area of kernels was used to classify touching and non-touching kernels, which the objects with a projected area more than 1.45 times the MVPA were considered to be touching objects, and the remaining objects were considered to be non-touching objects; (7) with those non-touching kernels, all pixels of all non-touching kernels were summed and divided by the number of those non-touching kernels, then multiplied by the spatial resolution (0.02295684 mm^2/pixel) would be the MVPA; all pixels of all non-touching kernels' edges were summed and divided
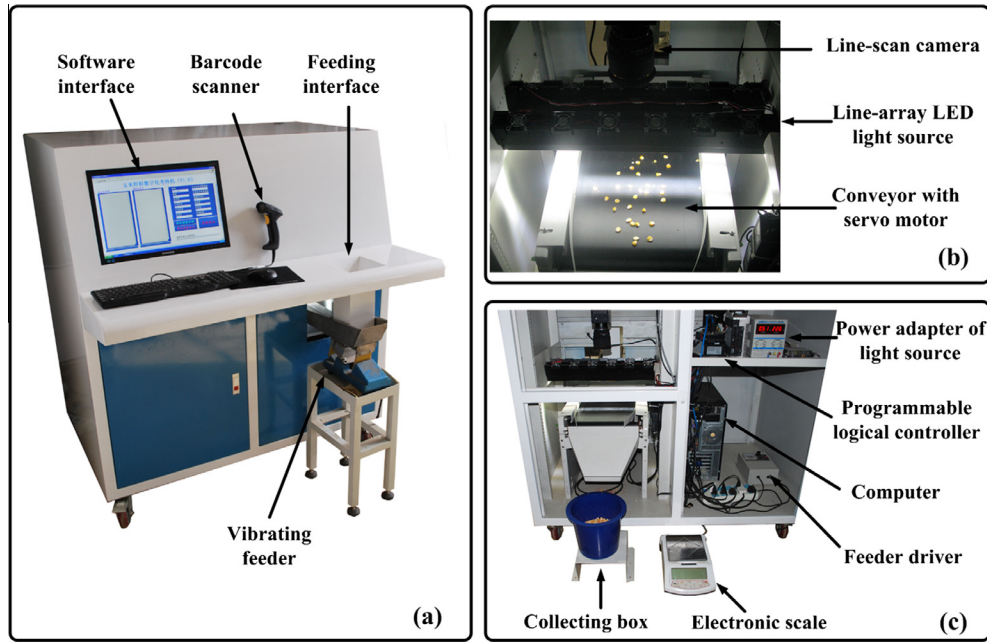
Fig. 1. The maize kernel traits scorer, (a) the user operation area and the system prototype; (b) the inspection unit; (c) the inner layout of the system.

by the number of those non-touching kernels, then multiplied by the spatial resolution (0.1515 mm/pixel) would be the MVPP; (8) each non-touching kernel was rotated with its rotation angle, which was defined as the angle of the line passing through the particle center of mass with the lowest moment of inertia and was calculated using the Eq. (1) with LabVIEW Sub VI (IMAQ Particle Analysis) (shown in Fig. 3f); the minimum enclosing rectangle (shown in Fig. 3f) was obtained; the average length of all minimum enclosing rectangles for all non-touching kernels multiplied by the spatial resolution (0.1515 mm/pixel) would be the mean kernel length, the average width of them multiplied by the spatial resolution would be the mean kernel width, and the ratio of the mean length to the mean width would be the mean kernel length-width ratio; (9) the projected areas of the touching objects were divided by the MVPA and the number of objects in touching image (denoted by $N2$) was obtained, along with the number of non-touching objects (denoted by $N1$), such that the number of all maize kernels (N_{Mk}) could be calculated based on the equation $N_{Mk} = N1 + N2$; (10) the TKW was obtained using an electronic scale, and the 100-KW was calculated using the Eq. (5).

$$\theta = \frac{1}{2} a \tan \left(\frac{2I_{xy}}{I_{xx} - I_{yy}} \right) \tag{1}$$

In Eq. (1), θ is the rotation angle; I_{xx} is the moment of Inertia xx and is calculated by Eq. (2); I_{xy} is the moment of Inertia xy and is calculated by Eq. (3); I_{yy} is the moment of Inertia yy and is calculated by Eq. (4).

$$I_{xx} = \sum x^2 - \frac{\left(\sum x \right)^2}{A} \tag{2}$$

$$I_{xy} = \sum xy - \frac{\sum x \cdot \sum y}{A} \tag{3}$$

$$I_{yy} = \sum y^2 - \frac{\left(\sum y \right)^2}{A} \tag{4}$$

In Eqs. (2)–(4), x is the x-coordinate of the foreground points in the kernel; y is the y-coordinate of foreground points in the kernel; A is the area of the kernel.

$$100\text{-KW} = \frac{\text{TKW} \times 100}{N_{\text{MK}}} \tag{5}$$

The key image analysis procedures are shown in Fig. 3. The original merged image is shown in Fig. 3a. The small particles (the white triangles in Fig. 3a) that were not maize kernels were removed (Fig. 3b). The results of the touching and non-touching particle assessments are shown in Fig. 3c and d, respectively. Each single particle was extracted (Fig. 3e) to calculate the kernel length and kernel width within the minimum enclosing rectangle (Fig. 3f). The source code for image processing was shown in the Supplementary file 4.

3. Results and discussion

3.1. Selection of the threshold value to distinguish touching kernels from non-touching kernels

To choose a threshold value to distinguish touching kernels from non-touching kernels, the misjudgment rate (MR, defined by Eq. (6)) distributions of KPA with different threshold values were analyzed using 65 samples chosen randomly from the 615 samples; the results are shown in Fig. 4. The minimum MR was obtained when the threshold value was set at 1.4 times the average projected area or 1.45 times the average projected area. We selected 1.45 times the average projected area as the optimal threshold value to distinguish non-touching kernels from touching kernels.

$$\text{MR} = \frac{n_1 + n_2}{n} \times 100\% \tag{6}$$

In Eq. (6), MR is the misjudgment rate, n_1 is the number of touching maize kernels that were falsely accepted as non-touching kernels, n_2 is the number of non-touching maize kernels that were falsely accepted as touching kernels, and n is the total number of kernels in the image which is acquired by counting maize kernels in the image manually.
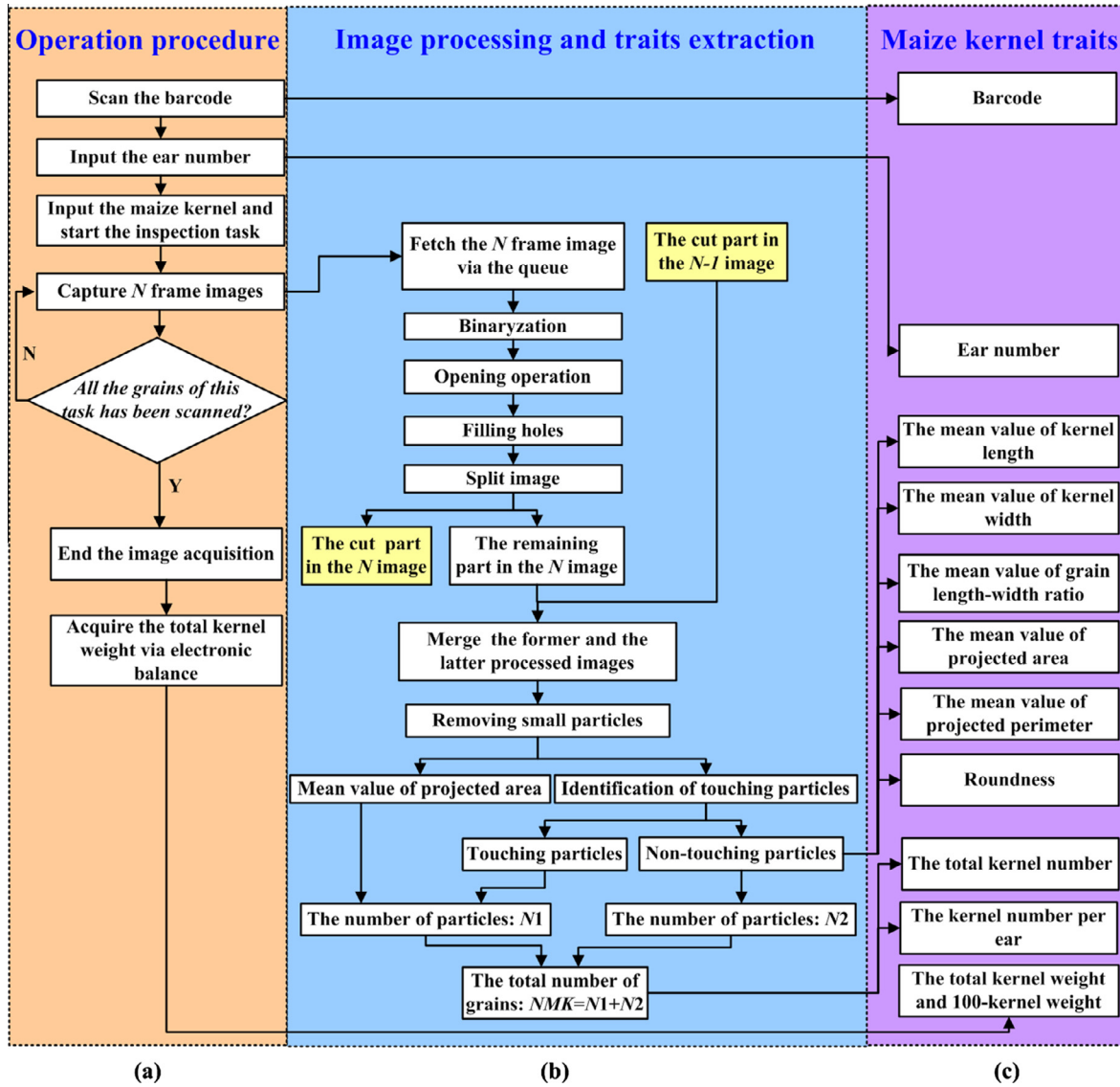
Fig. 2. The system operation procedure and image processing flow chart for the measurement of maize kernel traits, (a) the system operation procedure; (b) image processing and trait extraction flow chart; (c) maize kernel traits.

3.2. Accuracy of system measurements for KL, KW, LWR, and TKN

In total, 615 maize samples were automatically measured using the MKTS system. The frequency number plots for KL, KW, LWR, and TKN were shown in Fig. 5b, d, f, and h, respectively. The mean absolute percentage errors (MAPE, defined by Eq. (7)) for KL, KW, LWR, and TKN [7] were 1.24%, 2.24%, 2.58%, and 0.67%, respectively. The root mean squared error (RMSE, defined below by Eq. (8)) for KL, KW, LWR, and TKN were 0.15 mm, 0.23 mm, 0.04, and 2.26, respectively. The standard deviation of APE (STDEV$_{APE}$, defined by Eq. (9)) for KL, KW, LWR, and TKN were 1.09%, 1.73%, 2.02%, and 0.74%, respectively. The R^2 (the square of the correlation coefficient) for KL, KW, LWR, and TKN were 0.97, 0.96, 0.81, and 0.99, respectively.

The scatter plots for the automatic measurements versus the manual measurements for KL, KW, LWR, and TKN were shown in Fig. 5a, c, e, and g, respectively.

$$\text{MAPE} = \frac{1}{n} \sum_{i=1}^{n} \frac{|x_{ai} - x_{mi}|}{x_{mi}} \times 100\% \tag{7}$$

$$\text{RMSE} = \sqrt{\frac{1}{n} \sum_{i=1}^{n} (x_{ai} - x_{mi})^2} \tag{8}$$

$$\text{STDEV}_{\text{APE}} = \sqrt{\frac{\sum_{i=1}^{n} (\text{APE}_i - \text{MAPE})^2}{n - 1}} \tag{9}$$

In Eqs. (7)–(9), x_{mi} is the manually measured value; x_{ai} is the automatically measured value, n is the number of maize samples; APE$_i$ is the absolute percentage error of the i_{th} maize sample.

From the frequency number plots (Fig. 5b, d, and h), all absolute percentage errors for KL, KW, and TKN were less than 7%, 10%, and 5%, respectively. The measuring accuracy of maize kernel traits was shown in Table 1. The basic description statistics analysis of maize kernel traits was shown in Table 2, where the roundness is defined by Eq. (10). The closer the shape of a kernel was to a disk, the closer the roundness to 1. The MAPE of all maize kernel traits were within 3%.

$$\text{Roundness} = \frac{\text{Perimeter}}{\text{the ciucumference of a circle with the same area}} \tag{10}$$
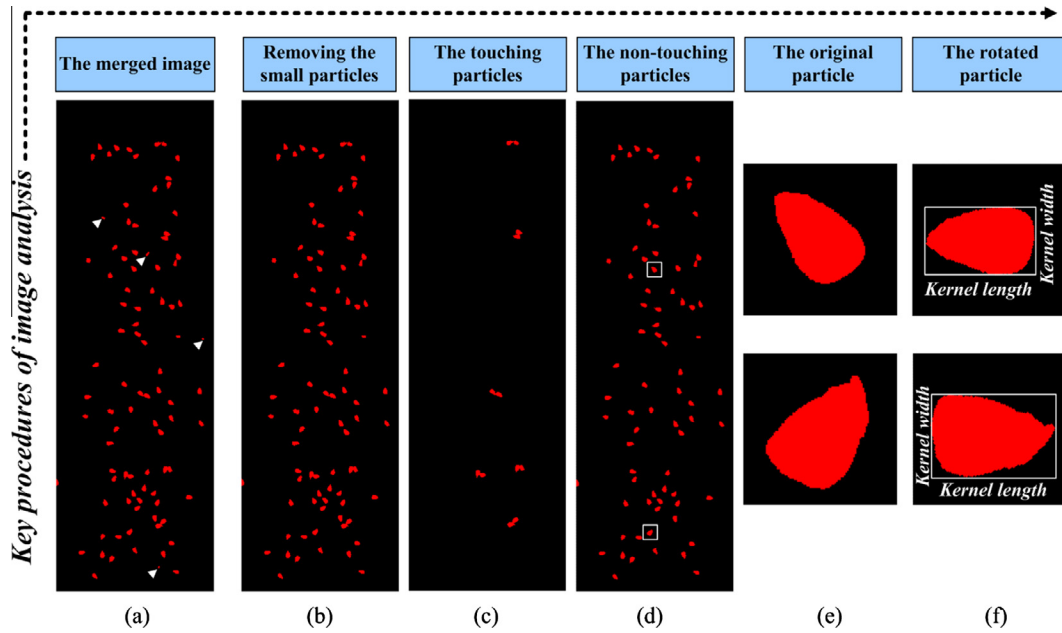
Fig. 3. The key image analysis procedures, (a) the original merged image; (b) the image after small particles were removed; (c) the results of the touching particles; (d) the results of the non-touching particles; (e) a selected single particle; (f) a rotated single particle.
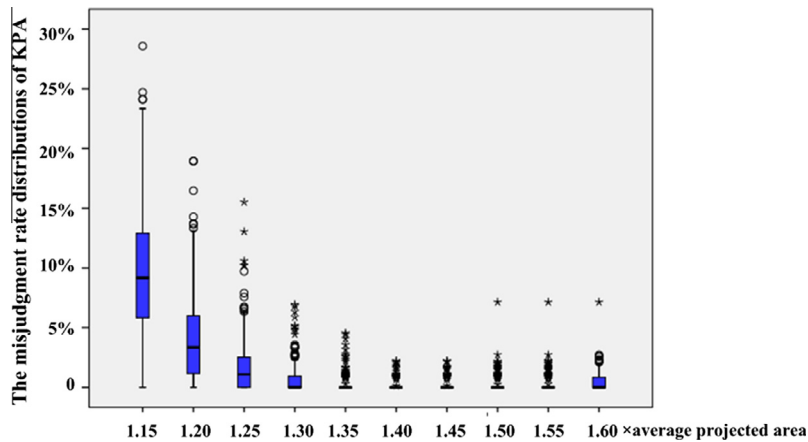

Fig. 4. The misjudgment rate (MR) distributions for KPA with different threshold values. Kernels with projected areas larger than the threshold value were considered to be touching kernels; all remaining kernels were considered to be non-touching kernels. '*' is the extreme outlier, '°' is the mild outliers.

3.3. Repeatability of system measurements

To evaluate the repeatability of system measurements, we randomly selected 10 kernels samples from 615 maize samples and measured all of the kernel traits ten times. The coefficients of variation (C.V) for all kernel traits were within 3%. The results were shown in Table 3.

$$E_x = \frac{1}{n}\sum_{i=1}^{n} x_{ai}$$

$$\text{C.V} = \frac{\sqrt{\frac{1}{n}\sum_{i=1}^{n}(x_{ai} - E_x)^2}}{E_x} \tag{11}$$

3.4. Measurement efficiency

If one worker operated the software, scanned the barcode and input the maize kernels, and another worker collected the maize kernels and pressed the print button on the electronic scale, the system would require approximately 72 s to measure 6 ears (when all kernels are input together at one time). If the system is run continuously for 24 h, the measuring efficiency would increase, up to 1200 samples per day. However, two experienced workers are required for approximately 540 s to manually measure 6 ears; this includes the counting and recording of all 12 traits, but not typing or correcting the data. From this point of view, the efficiency of the system was more than 7 times greater than that of manual operations at their maximum throughput.

4. Conclusions

Equipped with multidisciplinary techniques, including photonics, automatic controls and digital imaging processing, a maize kernel traits scorer (MKTS) was developed to measure 12 maize kernel traits. We evaluated the measurement accuracy and the repeatability of the system. We also demonstrated the use of the system to
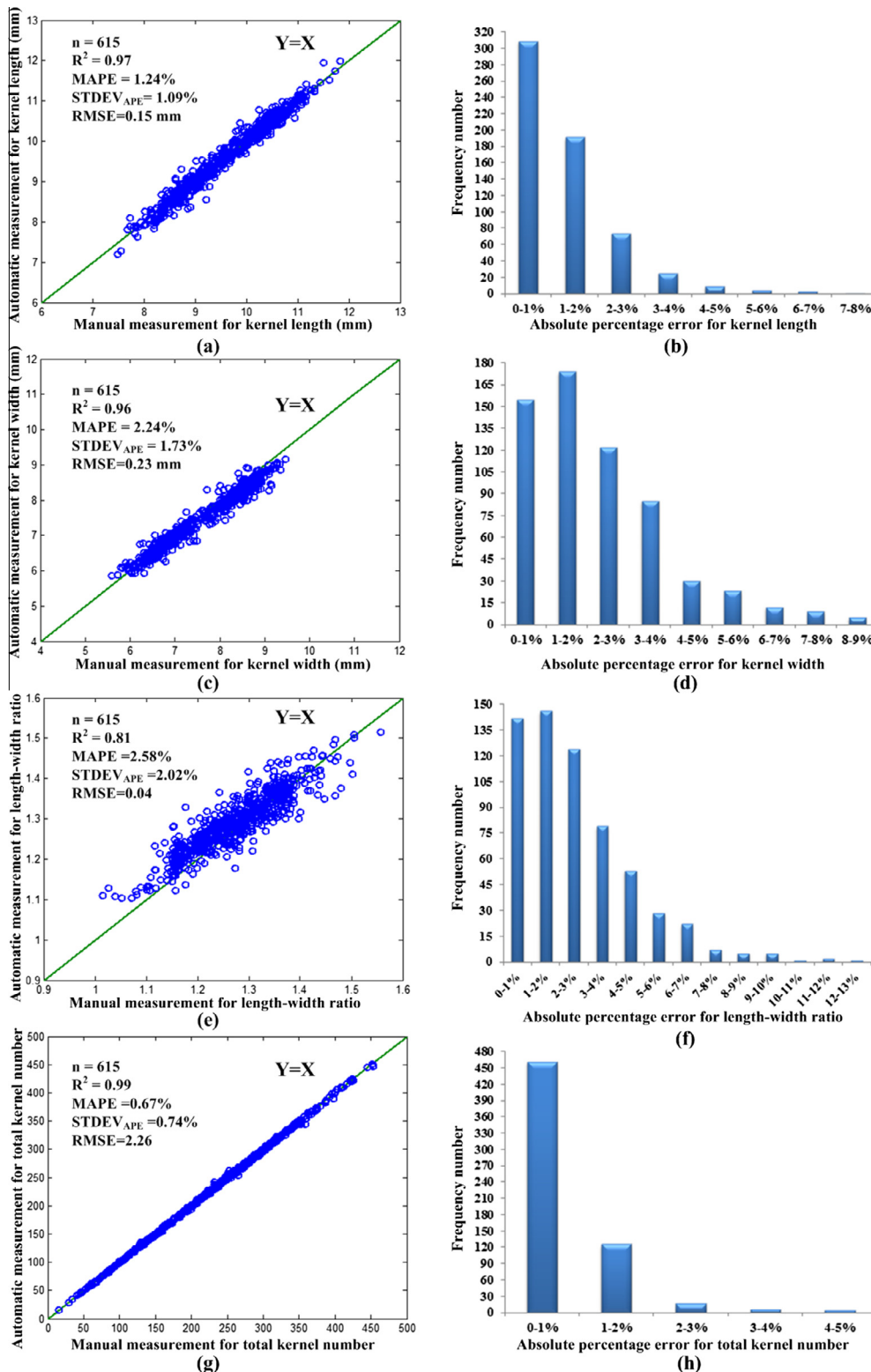
Fig. 5. Frequency number plots and scatter plots of the automatic measurements versus the manual measurements of maize kernel traits. (a) Scatter plots of the automatic measurements versus the manual measurements of kernel length; (b) frequency number plots for kernel length; (c) scatter plots of the automatic measurements versus the manual measurements of kernel width; (d) frequency number plots for kernel width; (e) scatter plots of the automatic measurements versus the manual measurements of kernel length-width ratio; (f) frequency number plots for kernel length-width ratio; (g) scatter plots of the automatic measurements versus the manual measurements of total kernel number; (h) frequency number plots for total kernel number.

facilitate the measurement of maize kernel traits. In the future, if maize kernel volume is obtained, the bulk density (defined as the weight of 1 liter volume of kernels) can also be calculated. Com-

pared with traditional phenotyping, MKTS provided the following three major advantages: automation, high-throughput and the absence of human disturbance. In conclusion, this high-accuracy

Table 1
Measurement accuracy for maize kernel traits.

Sample number	Kernel traits	R^2	RMSE	MAPE (%)	STDEV$_{APE}$ (%)	Frequency[a]			
						0–3%	3–5%	5–10%	More than 10%
615	KL (mm)	0.97	0.15	1.24	1.09	93.17%	5.53%	1.30%	0
	KW (mm)	0.96	0.23	2.24	1.73	73.33%	18.70%	7.97%	0
	LWR	0.81	0.04	2.58	2.02	66.99%	21.46%	10.89%	0.65%
	TKN	0.99	2.26	0.67	0.74	98.21%	1.79%	0	0

[a] Frequency of 0–3%: the ratio of samples whose APE was between 0% and 3%; Frequency of 3–5%: the ratio of samples whose absolute percentage error (APE) was between 3% and 5%; Frequency of 5–10%: the ratio of samples whose APE was between 5% and 10%; Frequency of more than 10%: the ratio of samples whose APE was more than 10%.

Table 2
The basic description statistics analysis of maize kernel traits for 615 samples.

Sample number	Statistics description	TKN	KL (mm)	KW (mm)	LWR	KPA (mm^2)	KPP (mm)	TKW (g)	100-KW (g)	Roundness
615	Range	16–451	7.19–11.98	5.86–9.15	1.10–1.51	30.34–67.18	20.36–30.59	3.30–132.30	10.53–33.67	1.03–1.10
	Mean	225.39	9.64	7.48	1.29	49.16	25.94	54.16	22.74	1.05
	STDEV	89.08	0.89	0.83	0.07	8.66	2.29	28.84	5.23	0.01

Table 3
Maize kernel traits for 10 samples (randomly selected from 615 samples) measured ten times.

Sample	Statistics	TKN	KL	KW	LWR	KPA	KPP	100-KW
1	STDEV	1.89	0.07	0.07	0.01	0.30	0.08	0.13
	C.V	0.59%	0.75%	0.85%	0.99%	0.58%	0.29%	0.59%
2	STDEV	1.34	0.09	0.07	0.01	0.42	0.12	0.09
	C.V	0.46%	0.94%	0.98%	0.88%	0.93%	0.46%	0.47%
3	STDEV	2.71	0.06	0.06	0.01	0.30	0.12	0.17
	C.V	0.85%	0.61%	0.84%	0.90%	0.64%	0.45%	0.85%
4	STDEV	1.96	0.09	0.06	0.02	0.43	0.11	0.13
	C.V	0.63%	0.95%	0.73%	1.44%	0.88%	0.44%	0.63%
5	STDEV	1.03	0.08	0.05	0.01	0.45	0.14	0.08
	C.V	0.44%	0.83%	0.74%	0.94%	1.02%	0.56%	0.44%
6	STDEV	2.04	0.09	0.06	0.02	0.53	0.19	0.14
	C.V	0.73%	1.00%	0.85%	1.31%	1.13%	0.76%	0.73%
7	STDEV	1.55	0.10	0.11	0.02	0.60	0.20	0.11
	C.V	0.49%	1.06%	1.47%	1.77%	1.18%	0.75%	0.49%
8	STDEV	1.06	0.04	0.05	0.01	0.39	0.11	0.08
	C.V	0.37%	0.42%	0.67%	0.81%	0.80%	0.42%	0.37%
9	STDEV	1.57	0.09	0.03	0.02	0.20	0.08	0.08
	C.V	0.50%	0.97%	0.50%	1.35%	0.47%	0.33%	0.50%
10	STDEV	1.18	0.07	0.05	0.01	0.36	0.09	0.11
	C.V	0.52%	0.69%	0.66%	0.94%	0.71%	0.31%	0.52%

C.V: coefficient of variation, which is defined by Eq. (11).

and high-throughput scorer will provide maize scientists with a novel tool to assist with research in maize genetics, functional genomics and breeding.

Appendix A. Supplementary material

Supplementary data associated with this article can be found, in the online version, at http://dx.doi.org/10.1016/j.measurement.2016.05.015.

References

[1] B.M. Prasanna, K. Pixley, M.L. Warburton, C.X. Xie, Molecular marker-assisted breeding options for maize improvement in Asia, Mol. Breeding 26 (2010) 339–356.

[2] X. Yang, S. Gao, Sh. Xu, Z. Zhang, B.M. Prasanna, L. Li, J. Li, J. Yan, Characterization of a global germplasm collection and its potential utilization for analysis of complex quantitative traits in maize, Mol. Breeding 28 (2011) 511–526.

[3] M. de Luna Alves Lima, C.L. De Souza Jr., D.A.V. Bento, A.P. De Souza, L.A. Carlini-Garcia, Mapping QTL for grain yield and plant traits in tropical maize population, Mol. Breeding 17 (2006) 227–239.

[4] C. Riedelsheimer, J.B. Endelman, M. Stange, M.E. Sorrells, J.L. Jannink, A.E. Melchinger, Genomic predictability of interconnected biparental maize populations, Genetics 194 (2013) 493–503.

[5] Z. Zhang, Z. Liu, Y. Hu, W. Li, Z. Fu, D. Ding, H. Li, M. Qiao, J. Tang, QTL analysis of kernel-related traits in maize using an immortalized F2 population, PLoS ONE 9 (2) (2014) e89645.

[6] B. Peng, Y. Li, Y. Wang, C. Liu, Z. Liu, W. Tan, Y. Zhang, D. Wang, Y. Shi, B. Sun, Y. Song, T. Wang, Y. Li, QTL analysis for yield components and kernel-related traits in maize across multi-environments, Theor. Appl. Genet. 122 (2011) 1305–1320.

[7] L. Duan, W. Yang, C. Huang, Q. Liu, A novel machine-vision-based facility for the automatic evaluation of yield-related traits in rice, Plant Methods 7 (44) (2011).

[8] H.K. Mebatsion, J. Paliwal, A fourier analysis based algorithm to separate touching kernels in digital images, Biosyst. Eng. 108 (2011) 66–74.

[9] K.K. Patel, A. Kar, S.N. Jha, M.A. Khan, Machine vision system: a tool for quality inspection of food and agricultural products, J. Food Sci. Technol. 49 (2) (2012) 123–141.

[10] W. Yang, L. Duan, G. Chen, L. Xiong, Q. Liu, Plant phenomics and high-throughput phenotyping: accelerating rice functional genomics using multidisciplinary technologies, Curr. Opin. Plant Biol. 16 (2) (2013) 180–187.

[11] Ch. Huang, W. Yang, L. Duan, N. Jiang, G. Chen, L. Xiong, Q. Liu, Rice panicle length measuring system based on dual-camera imaging, Comput. Electron. Agric. 98 (2013) 158–165.

[12] K. Liao, M.R. Paulsen, J.F. Reid, Real-time detection of color and surface defects of maize kernels using machine vision, J. Agric. Eng. Res. 59 (4) (1994) 263–271.

[13] M. Tanska, D. Rotkiewica, W. Kozirok, I. Konopka, Measurement of the geometrical features and surface color of rapeseeds using digital image analysis, Food Res. Int. 38 (2005) 741–750.

[14] M. Wiwart, E. Suchowilska, W. Lajszner, L. Graban, Identification of hybrids of spelt and wheat and their parental forms using shape and color descriptors, Comput. Electron. Agric. 83 (2012) 68–76.

[15] B. Ni, M.R. Paulsen, K. Liao, J.F. Reid, Design of an automated corn kernel inspection system for machine vision, Trans. ASAE 40 (2) (1997) 491–497.

[16] H.F. Ng, W.F. Wilcke, R.V. Morey, J.P. Lang, Machine vision evaluation of corn kernel mechanical and mould damage, in: 1997 ASAE Annual International Meeting Technical Pagers, Paper No. 973047, ASAE, 2950 Niles Road, St. Joseph, Michigan 49085-9659, USA.

[17] E.R. Davies, M. Bateman, D.R. Mason, J. Chambers, C. Ridgway, Design of efficient line segment detectors for cereal grain inspection, Pattern Recogn. Lett. 24 (2003) 413–428.

[18] F. Breseghello, M.E. Sorrells, Association mapping of kernel size and milling quality in wheat (*Triticum aestivum* L.) cultivars, Genetics 172 (2) (2006) 1165–1177.

[19] Y.N. Wan, C.M. Lin, J.F. Chiou, Rice quality classification using an automatic grain quality inspection system, Trans. ASAE 45 (2) (2002) 379–387.

[20] A. Pazoki, F. Farokhi, Z. Pazoki, Corn seed varieties classification based on mixed morphological and color features using artificial neural networks, Res. J. Appl. Sci. Eng. Technol. 6 (19) (2013) 3506–3513.

[21] Y.N. Wan, Kernel handling performance of an automatic grain quality inspection system, Trans. ASAE 45 (2) (2002) 369–377.

[22] M.R. Paulsen, W.D. Wigger, J.B. Litchfield, J.B. Sinclair, Computer image analyses for detection of maize and soybean kernel quality factors, J. Agric. Eng. Res. 43 (1980) 93–101.

[23] B.P. Dubey, S.G. Bhagwat, S.P. Shouche, J.K. Sainis, Potential of artificial neural networks in varietal identification using morphometry of wheat grains, Biosyst. Eng. 95 (1) (2006) 61–67.

[24] J.M. Valiente-Gonzalez, G. Andreu-Garcia, P. Potter, A. Rodas-Jorda, Automatic corn (*Zea mays*) kernel inspection system using novelty detection based on principal component analysis, Biosyst. Eng. 117 (SI) (2014) 94–103.

[25] Y. Xun, J. Zhang, W. Li, W. Cai, Multi-objective dynamic detection of seeds based on machine vision, Prog. Nat. Sci. 17 (2) (2007) 217–221.

[26] L. Steenhoek, C. Precetti, Vision sizing of seed corn, in: 2000 ASAE Annual International Meeting, Paper No.003095, ASAE, 2950 Niles Road, St.Joseph, Michigan 49085-9659, USA.

[27] B. Ni, M.R. Paulsen, J.F. Reid, Size grading of corn kernels with machine vision, in:1997 ASAE Annual International Meeting Technical Pagers, Paper No.973046, ASAE, 2950 Niles Road, St. Joseph, Michigan 49085-9659, USA.

[28] A.D. Severini, L. Borrás, A.G. Cirilo, Counting maize kernels through digital image analysis, Crop Sci. 51 (2011) 2796–2800.

[29] C. Igathinathane, L.O. Pordesimo, E.P. Columbus, W.D. Batchelor, S.R. Methuku, Shape identification and particles size distribution from basic shape parameters using ImageJ, Comput. Electron. Agric. 63 (2008) 168–182.

[30] T. Tanabata, T. Shibaya, K. Hori, K. Ebana, M. Yano, SmartGrain: high-throughput phenotyping software for measuring seed shape through image analysis, Plant Physiol. 160 (2012) 1871–1880.